



# Hydrogen in Gas Grids

**A systematic validation approach at various admixture levels into high-pressure grids**

## D4.2 Report on results of the validation

**Date** 25 October 2022 (M34)  
**Grant Number** 875091  
**Author(s)** **Virginia Madina**<sup>1</sup>, Jorge Aragón,<sup>1</sup> Ekain Fernanández,<sup>1</sup> Vanesa Gil<sup>2,3</sup>, Javier Sánchez<sup>2</sup>, Alberto Cerezo<sup>4</sup>

1 Tecnalia  
 2 FHA  
 3 ARAID  
 4 Redexis

Author printed in bold is the contact person

**Status** Started / Draft / Consolidated / Review / **Approved** / Submitted / Accepted by the EC / Rework [use bold style for current state]

**Dissemination level:**

**PU** Public

**RE** Restricted to a group specified by the consortium\*

**PP** Restricted to other programme participants\*

**CO** Confidential, only for members of the consortium\*

\*(including the Commission Services)



This project has received funding from the Fuel Cells and Hydrogen 2 Joint Undertaking (now Clean Hydrogen Partnership) under Grant Agreement No. 875091 'HIGGS'. This Joint Undertaking receives support from the European Union's Horizon 2020 Research and Innovation program, Hydrogen Europe and Hydrogen Europe Research.

## Document history

Version	Date	Description
1.1	2022-09-28	First draft
1.2	2022-09-30	Revised
1.3	2022-10-24	Consolidated version
1.4	2022-10-26	Final version

The contents of this document are provided “AS IS”. It reflects only the authors’ view and the JU is not responsible for any use that may be made of the information it contains.

# Table of Contents

**Document history** .....2

**Executive Summary** .....6

**1 Objective** .....7

**2 Introduction**..... 8

**3 Test methods for the testing platform at FHa**..... 9

3.1 Gas tightness tests ..... 9

3.2 Hydrogen sensitivity tests ..... 10

3.3 Gas separation test..... 14

**4 Results of the first experimental campaign** ..... 16

4.1 Gas tightness tests ..... 16

4.2 Hydrogen sensitivity tests ..... 17

4.2.1 API 5L constant strain specimens ..... 17

4.2.2 Inspection of equipment from the dynamic section ..... 21

4.2.3 Inspection of equipment from the static section..... 24

4.3 Gas separation performance of the membrane prototype ..... 25

**5 Results of the second experimental campaign** ..... 27

5.1 Results of gas tightness tests..... 27

**6 Conclusions** ..... 30

**Bibliography and References**..... 31

**Acknowledgements** .....32

## List of Figures

Figure 1. Layout of HIGGS experimental platform.....	9
Figure 2. Optical micrograph showing detail of cross section of GTA welded joint in X70 steel (left) and micro-hardness evolution in this welded joint (right) .....	11
Figure 3. Picture of the pig trap (left) and the constant strain specimens allocated inside it (right) .....	12
Figure 5. Evolution of the pressure (left) and gas composition in %mol H <sub>2</sub> (right) in each line of the static section during the first experimental campaign .....	17
Figure 6. Test specimens inside the pig trap in the loop experimental platform at FHA at the beginning of the test, and once concluded .....	18
Figure 7. Detail of tested C-ring specimens.....	18
Figure 8. Optical micrographs of notched C-ring sections from steel grades X70 (left) and X42 (right) .....	19
Figure 9. (up-left) detail of 4pb X70 welded steel specimens; (up-right) metallographic probe of welded sections; (down) optical micrographs of welded joints from steel grades X52 (left) and X70 (right) .....	19
Figure 10. Detail of rack with tested CT bolt loaded specimens .....	20
Figure 11. (up left) two heat tinted fracture surfaces in a X70 CT-WOL tested specimen; (up right) detail of the tinted fatigue precrack; SEM micrographs of the fracture surface in the fatigue pre-crack and in the crack front .....	20
Figure 12. Parts of the pressure regulator: membrane: general appearance (left), detail of area with unknown damaged area (center) and cross section materialographic probe (right) showing a very superficial damage.....	21
Figure 13. Parts of the regulator: gasket (left) and guide rings (right) .....	22
Figure 14. Parts of the regulator: metallic gasket .....	22
Figure 15. Pre-pilot: O-ring (left), filter cartridge (center) and pad (right) .....	22
Figure 16. Pilot: membranes and guided rings (right) and detail of membrane .....	23
Figure 17. Pilot guide ring (left) and pilot metallic obturator.....	23
Figure 18. Filter cartridge .....	23
Figure 19. Spirometallic gaskets .....	23
Figure 20. Butterfly valve seal.....	24
Figure 21. Flanged ball valve C-V-17. Detail of teflon seals (left) and graphoil body seals (center and right) .....	24
Figure 22. Detail of teflon and graphoil seals in flanged ball valve C-V-15 (left) and C-V-16 (right).....	24
Figure 23. Detail of teflon and graphoil seals in DIDTEK butterfly valve seal.....	25
Figure 24. Gas separation performance of the prototype with Membrane #1. Blue line stands for the total permeate flow and orange scatter stands for the H <sub>2</sub> purity in the permeate stream. ....	25
Figure 25. Evolution of the pressure (left), the P/Z·T quotient (middle) and gas composition in %mol H <sub>2</sub> (right) in each line of the static section during the second experimental campaign.....	28

## List of Tables

Table 1. List of valves tested in the R&D facility.....	10
Table 2. Testing elements in the dynamic section of the testing platform (“pseudo” Metering and Regulation Station) .....	10
Table 3. Properties of API5L steel pipes under study .....	11
Table 4. Estimated maximum value of K <sub>IAPP</sub> and K <sub>IC</sub> for the HIGGS’ CT-WOL specimens.....	13

## D4.2 Report on results of the validation

---

Table 5. Types of constant displacement specimens used in the testing platform and summary conditions .....	14
Table 6. Results of CT-WOL specimens testing.....	21
Table 7. Gas separation performance of the Membrane #2 for the tests under: (top part) same feed low and variable feed pressure; (bottom part) variable feed flow and feed pressure with the aim at maximizing the hydrogen recovery factor .....	26
Table 8. Schedule of the experimental campaign.....	27

## Executive Summary

Deliverable D4.2 gathers the results obtained in the different tests performed during the first and second experimental campaigns, carried out in the R&D testing platform built in WP3 at Fundación Hidrógeno Aragón (FHA). This R&D facility aims to reproduce a natural gas transport grid at smaller scale, where different testing components, materials and equipment are exposed to hydrogen. Three different kinds of tests have been performed:

- Gas tightness tests of representative valves of the natural gas (NG) grid to identify possible leakages when operated with hydrogen. The tested valves have been besides thereafter inspected for hydrogen damage.
- Constant strain tests carried out on API 5L steel specimens' grades X42 to X70, for hydrogen embrittlement evaluation on representative carbon steels in the grid.
- H<sub>2</sub>/CH<sub>4</sub> gas separation tests with a Pd-based membrane prototype, thinking in potential end-users that demand a high natural gas purity and want to remain being costumers of the grid when natural gas comes blended with hydrogen.

The first experimental campaign has consisted in the 20/80 (%/%vol) H<sub>2</sub>/CH<sub>4</sub> blend gas condition, without impurities, at 80 bar for 3000 hours. The tightness of different kind of valves led to hydrogen losses below 1 Nml·h<sup>-1</sup>. No cracks or other kind of damage was found on parts of the equipment (regulator, flowmeter) exposed to the H<sub>2</sub>/CH<sub>4</sub> blend. C-ring, 4pb and CT-WOL specimens machined from API5L steel pipes grades X42 to X70, did not show cracking or pre-crack growth after testing in the hydrogen blend. Besides, H<sub>2</sub>/CH<sub>4</sub> separation has also been successfully achieved using Pd-based membrane technology, obtaining a high-purity methane stream. The tested elements have shown therefore compatibility to this hydrogen level under the specific conditions considered.

Finally, some preliminary results of the second experimental campaign are also included in this report. Specifically, those corresponding to the gas tightness tests. In this last campaign, the 20/80 (%/%vol) H<sub>2</sub>/CH<sub>4</sub> blend has also been used but including up to 11 ppmv of H<sub>2</sub>S and 4%mol CO<sub>2</sub> as impurities, to check the effect of the most common impurities in NG. It was not possible to assess the tightness of the flanged testing valves because of their manipulation after the first experimental campaign, concluding that any manipulation on this kind of components should be done only by the manufacturer. The tightness of the flanged and screwed couplings and of the screwed testing valves, have also been assessed with positive results. However, a failure found in one screwed ball valve after emptying the platform makes necessary its full characterization to reach better conclusions.

# 1 Objective

The main objective of this deliverable is to gather and discuss the results obtained in the first testing campaign carried out in the R&D testing platform developed in WP3 at FHA, as well as the preliminary results of the second campaign.

More specifically, the objectives of the tests carried out in this campaign operating at 80 bar with a H<sub>2</sub>/CH<sub>4</sub> blend with 20% mol H<sub>2</sub> content, for 3000 hours, are:

- To check the tightness of representative valves of the NG grid.
- To evaluate a potential hydrogen embrittlement damage in API5L base and welded steel pipes, and other significant components and equipment of the NG gas grid.
- To check the long-term gas separation performance of a Pd-based membrane prototype.

## 2 Introduction

Blending hydrogen with NG may have an impact on safety issues, pipeline integrity, and gas quality. The potential leakage rate of hydrogen is much larger than that of NG through the same sized leak. Besides, possible hydrogen embrittlement mechanism may occur under the transport pressures and the combustion properties change when hydrogen is added to NG, with direct impact on end users.

Research to assess the impact of hydrogen on the NG infrastructure is therefore necessary when analysing its suitability for hydrogen transport, with special focus on hydrogen embrittlement and gas leakage. Gas separation technologies are also necessary to obtain high-concentrated methane streams from admixture flows below 20%mol H<sub>2</sub>.

Hydrogen embrittlement is a process in which the tensile ductility of a material working on hydrogen environment is significantly reduced because of the introduction of hydrogen atoms in its lattice. Additionally, the fracture toughness and fatigue strength of this material decreases. The severity of these manifestations of hydrogen embrittlement depends on mechanical, environmental and material (microstructure and tensile strength, principally) variables. It is critical to ensure the resistance of pipelines materials and other metallic materials in the grid to this phenomenon, for a safe and efficient hydrogen transport.

The testing platform built at FHA is an R&D setup that tries to replicate a transport NG facility in which real pipes, components and equipment of high-pressure grids have been installed to expose them to hydrogen blends at 80 bar pressure, to assess the suitability of high-pressure NG grids for the transport of H<sub>2</sub>/NG blends or even 100% H<sub>2</sub> gas. For this purpose, gas tightness tests, constant strain mechanical tests and gas permeation tests are carried out in the HIGGS project.



### 3 Test methods for the testing platform at FHa

This section describes the experiments that are being performed in the R&D platform designed and built within WP3. As reported in D 3.1 and D 3.3, the testing platform consists in a static section, a dynamic section and a membrane prototype. The tests that are currently carried out in each of them are explained in the following subsections. Figure 1 shows the layout of HIGGS experimental platform as shown in deliverable D3.4.

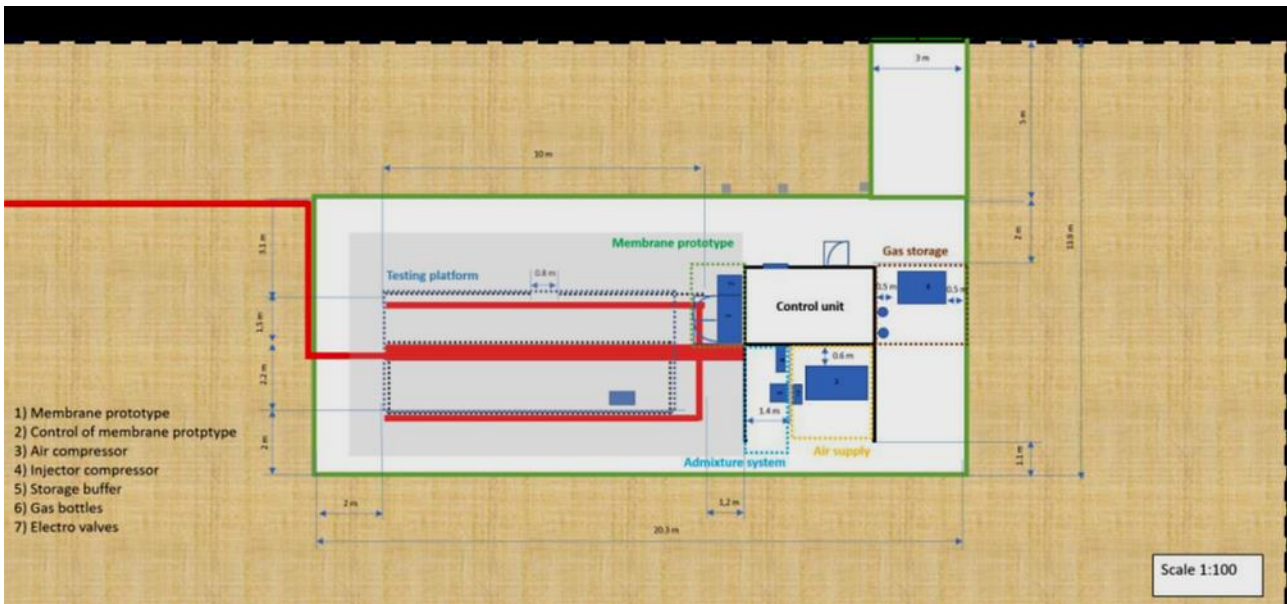


Figure 1. Layout of HIGGS experimental platform

#### 3.1 Gas tightness tests

The tightness of several valves towards hydrogen has been tested in the static section of the testing platform. Plug, needle, ball, and butterfly valves were selected in WP3 as the most representative valves in the grid, and they have been installed in the platform with flanged and screw couplings. In each line of the static section up to three testing valves can be installed. Each line is equipped with a pressure transmitter and an analysis port to monitor the pressure level and the hydrogen concentration in the line during the test, respectively.

The lines were fed at 80 bar and isolated afterwards. The lines stayed in a static way full of gas for 3000 h. During the test, the pressure was monitored, and the admixture composition checked periodically using a gas analyzer. Specific information about the testing valves can be seen in Table 1.

**Table 1. List of valves tested in the R&D facility**

Element	Manufacturer	Model	Connection (size and technical standard)	Additional comments
Ball Valve	ALFA VALVOLE	ALFA-606/FB Split Body	RF-3"	ANSI 600# Lever
Lug-type butterfly Valve	DIDTEK	LUG – ZERO LEAKAGE CLASS	RF-3"	ANSI 600# Gearbox & handwheel
Plug valve	KURVALF	RF-VP	RF-3"	ANSI 600# Lever
Needle valve	ALFA VALVOLE	ALFA-20T/FB S.800	thread ½"	ANSI 600#
Ball valve	NUOVAFIMA	BSV/VV	thread ½" NPT M x ½" NPT F	ANSI 600#

At the end of the test, the flanged valves were disassembled, and their different parts inspected to detect the presence of cracks or any other damage, that could be attributed to hydrogen exposure.

### 3.2 Hydrogen sensitivity tests

Potential damage due to hydrogen embrittlement on API 5L base and welded steel pipes and equipment of the NG grid has been studied in the dynamic section of the testing platform. The testing items were installed in a closed piping loop that works at 60-80 bar, under a constant flow of gas provided by a gas compressor together with the action of a pressure regulator. As testing equipment, a filter, a pressure regulator and a gas meter have been installed, building a kind of Metering and Regulation Station of the transmission grid. The characteristics of this equipment is given in Table 2. The equipment was working at 80 bar for 3000h exposed to the 20%mol H<sub>2</sub> blend. At the end of the test, all the items were disassembled and their different parts (springs, membranes, O-rings, etc.) inspected to detect the presence of cracks or any other damage.

As testing pipes, steels of different API 5L qualities (grades X42, X52, X60 and X70) have been selected. The as received chemical composition, mechanical properties and metal microstructure of the base and welded steels has been well characterized and collected in deliverables D3.1 and D4.1. Table 3 summarizes important aspects of the steels under study. The HAZ and weld metal regions corresponding to a X70 steel weld joint are shown in Figure 2, together with the hardness evolution in the above-mentioned regions.

**Table 2. Testing elements in the dynamic section of the testing platform (“pseudo” Metering and Regulation Station)**

Element	Manufacturer	Model	Connection (size and technical standard)	Additional comments
Cartridge Filter	FIORENTINI	HFA/1	RF-1"	ANSI 600#
Pilot-operated pressure regulator	FIORENTINI	REFLUX-819 P.207/A+R14 SB-105	RF-1"	ANSI 600#

## D4.2 Report on results of the validation

Element	Manufacturer	Model	Connection (size and technical standard)	Additional comments
Turbine flow meter	ELSTER	TR22 G100 A1R/A 1S	RF-3"	ANSI 600#
Pressure indicator	NUOVAFIMA	MGS18/2/A	thread 1/2" NPT-M	DN 100 KL0,6% 0-100 bar
Pressure Transmitter	YOKOGAWA	EJA530E-JCS7N-014EN /KU22	thread 1/2" NPT-M	0-100 bar 4-20 mA Display
Temperature transmitter	YOKOGAWA	YTA610	-	PT100 Sensor -50 +200 °C Display

**Table 3. Properties of API5L steel pipes under study**

API 5L steel grade	Nominal diameter (in)	Outside diameter (mm/in)	Wall thickness (mm) <sup>1</sup>	Yield strength (MPa)		Ultimate tensile strength (MPa)		Welding procedure /filler material	Microstructure (base steel)
				Tensile testing (ISO 6892) <sup>2</sup> [1]	API 5L (min.)	Tensile testing (ISO 6892)	API 5L (min.)		
X42	6	168.3 / 6.625	6.9	451	290	542	415	GTAW <sup>3</sup> / ER70S-6	Ferrite + pearlite
X52	6	168.3 / 6.625	7.8	440	360	514	460	GTAW / ER70S-6	Ferrite + pearlite
X60	6	168.3 / 6.625	7.8	510	415	581	520	GTAW / ER90S-B3	Bainite
X70	16	406.4 / 16.0	8.2	549	485	675	570	GTAW / ER90S-B3	Ferrite + bainite

<sup>1</sup> thickness obtained from metallographic cross sections

<sup>2</sup> average values of two tensile tests

<sup>3</sup> Gas Tungsten Arc Welding (GTAW)

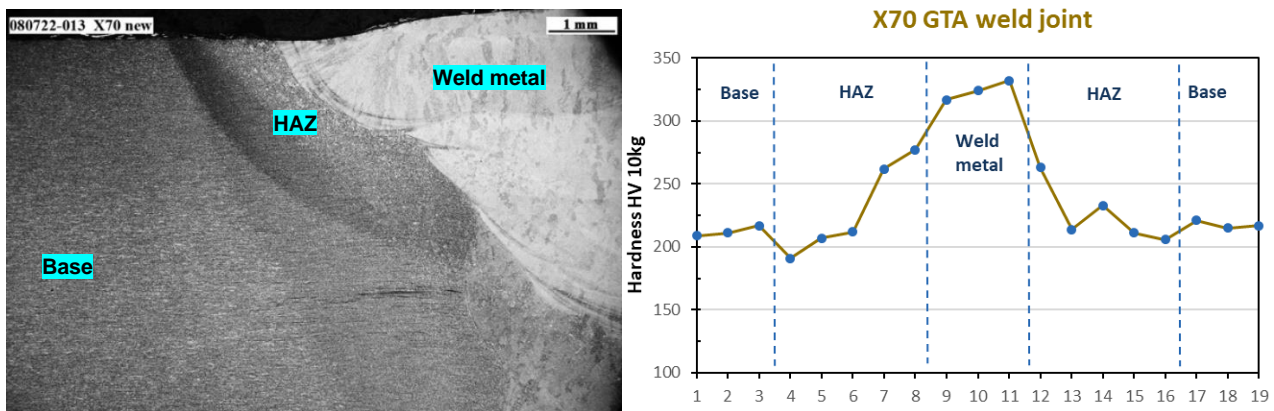


**Figure 2. Optical micrograph showing detail of cross section of GTA welded joint in X70 steel (left) and micro-hardness evolution in this welded joint (right)**

The tests on steels have been performed using constant displacement (or constant strain) specimens mechanized from the base and welded API 5L steel pipes shown in Table 3. The displacement initially applied to the specimen is held constant throughout the duration of the test. An important

## D4.2 Report on results of the validation

benefit of using constant strain specimens is that once the deformation has been applied to the specimen, the self-loading assemblies may be inserted into loops or closed test vessels and exposed to the hydrogen environment at a certain pressure. For this reason, a pig trap was installed in the dynamic section of the testing platform, aiming as an autoclave that can operate at 80 bar and in which the specimens have been allocated for the test. Three types of normalized constant displacement specimens have been developed in this work: C-ring, four-point bend (4pb) and compact tension (CT) wedge opening load (WOL) specimens. These specimens have been exposed to the 20%mol H<sub>2</sub> blend at 80 bar for 3000h inside the pig trap (Figure 3)



**Figure 3. Picture of the pig trap (left) and the constant strain specimens allocated inside it (right)**

C-rings specimens are made from tubular products and are bolt loaded to the desired stress level, usually comprised between 75 and 100% of the yield strength. Due to the circumferential welding of the pipe sections, C-ring specimens have only been machined out from base X42, X52 and X60 (OD 6"). It has been not possible to produce C-rings specimens from the X70 16" OD pipe. The thickness of the C-ring specimens is determined by the wall thickness of the as-received tube. The design, machining and loading process for C-ring specimens has been carried out according to ISO 7539-5 [2] and ASTM G38 [3] standards.

4pb specimens shall be flat strips of metal of uniform rectangular cross section and uniform thickness, except in the case of testing welded specimens where testing is specified with one face in the as-welded condition, for which a non-uniform cross section is inherent (see Figure 8). The 4pb specimen is subjected to a constant displacement that is performed by supporting the beam specimen on two loading rollers and applying a load through two other rollers, so that one face of the specimen is in tension and the other is in compression. Similar to the C-ring specimens, the stress level is comprised between 75 and 100% of the elastic limit. Base and welded 4pb specimens have been used in the 20%mol H<sub>2</sub> blend tests. The welded specimens were taken transverse to the circumferential weld, with the weld bead at the center of the specimen. Indications for the preparation and use of 4pb specimens are given in ISO 7539-2 [4] and ASTM G39 [5] standards. More information related with the equations used for estimating the deflection necessary to obtain the desired strain on the C-ring and 4pb specimens, can be found in deliverable D4.1.



## D4.2 Report on results of the validation

For C-ring and 4pb specimens the evaluation of the steel resistance to hydrogen embrittlement is realized by visual examination at the conclusion of the tests, for crack detection, followed by metallographic examination of cross sections.

The CT-WOL specimen is a compact geometry described in ASTM E1681 [6] that is well suited for constant displacement tests. The CT-WOL fatigue-precracked specimen can be self-loaded by tightening a bolt against a taper pin, to produce a constant displacement at the loading points. The maximum stress intensity factor ( $K_{IAPP}$ ) applied to the CT-WOL specimen can be estimated according to ASTM E1681. Estimated maximum values of  $K_{IAPP}$  and  $K_{IC}$  for the X52 and X70 CT-WOL specimens are shown in Table 4.

**Table 4. Estimated maximum value of  $K_{IAPP}$  and  $K_{IC}$  for the HIGGS' CT-WOL specimens**

Steel grade	Thickness (mm)	$K_{IC}$ max. [MPa $\sqrt{m}$ ]	$K_{IAPP}$ max. [MPa $\sqrt{m}$ ]
X52	6.6	22.1	51.8
x70	7.0	28.1	65.9

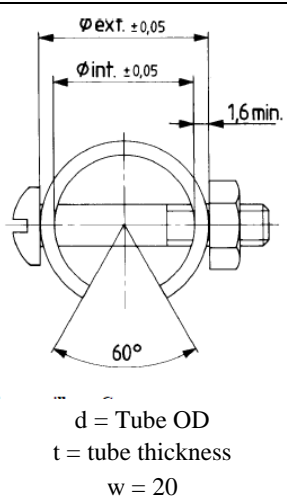
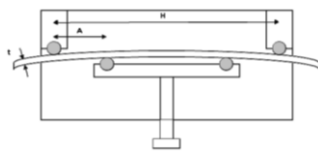
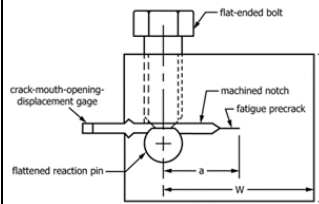
Indications for the preparation and use of these specimens are given in ISO 7539-6 [7], ASTM E1681 and ASTM E399 [8] standards.

The CT-WOL specimen is fatigue precracked in air according to ASTM E1681 section 7.3.4. Fatigue crack lengths of approximately 2 mm are sought. The force (P) to be applied is calculated from the selected  $K_{IAPP}$  and the measured pre-crack length, according to ASTM E1681.

The CT-WOL specimen is kept in the loaded condition for a specific time in the hydrogen gas blend. At the conclusion of the test, the CT-WOL specimens are unloaded and heat tinting (300 °C for 30 minutes). The CT specimen is broken, and the fracture surface is examined by SEM to assess if subcritical cracking occurred from the initial fatigue pre-crack. Measurements of the crack front extent are taken in three positions and the average crack growth in hydrogen is calculated. According to ASTM E1681 standard, there is no fatigue pre-crack growth if the average measured crack growth does not exceed 0.25 mm.

Three base specimens and two HAZ specimens of each of the steel grades X52 and X70, have been produced for the 20%mol H<sub>2</sub> blend tests. In the HAZ specimens, the notch is machined approximately normal to the surface of the material and in such manner that the pre-crack includes as much HAZ material as possible in the resulting fracture. The machined notch is oriented in the TL (transversal-longitudinal) direction, following indications of ASTM E399 standard. The thickness of the CT-WOL specimens is determined by the wall thickness of the as-received X52 and X70 steel pipes. Details of the three normalized constant displacement specimens are summarized in Table 5.

**Table 5. Types of constant displacement specimens used in the testing platform and summary conditions**

Type of specimen	Constant displacement specimens		
	C-ring	Four-point bend (4-pb)	CT-WOL
<b>Condition</b>	smooth and notched base specimens	Smooth base and welded specimens	Notched pre-cracked base and welded specimens
<b>Applicable standards</b>	ISO 7539-5, ASTM G 38	ISO 7539-2, ASTM G 39	ISO 7539-6, ASTM E1681, ASTM E399
<b>Specimen geometry</b>	 <p> <math>\phi_{ext.} \pm 0,05</math>  <math>\phi_{int.} \pm 0,05</math>            1,6 min.            60°  <math>d = \text{Tube OD}</math>  <math>t = \text{tube thickness}</math>  <math>w = 20</math> </p>	 <p> <math>H = 100</math>  <math>w = 10</math>  <math>t = \text{thickness} = 5-6</math> </p>	 <p> <math>t = \text{greatest thickness allowed by the bent and thickness of the pipe (at least 85\% of the pipe thickness)}</math> </p>
<b>Steel grades</b>	X42, X52, X60	X52, X70	X52, X70
<b>Environment</b>	20% mol H <sub>2</sub> in CH <sub>4</sub> (80 bar)		
<b>Test duration</b>	3000 hours		
<b>Post testing evaluation</b>	<ul style="list-style-type: none"> <li>- Evidence of cracking in C-ring and 4-pb specimens</li> <li>- Crack growth in CT-WOL specimens</li> <li>- Metallographic/fractographic examination by optical and SEM microscopy</li> </ul>		

### 3.3 Gas separation test

As explained in previous deliverables in WP3, membrane technology is being used in HIGGS to deal with H<sub>2</sub>/CH<sub>4</sub> separation. Pd-based double-skinned membranes deposited onto 14 mm OD porous ceramic tubes have been prepared and integrated in the membrane prototype for this study, following the preparation procedure reported in [9]. The first campaign was carried out by using Membrane #1 with 22.1 cm long and the second testing campaign by using Membrane #2 of 21.7 cm long. Pd-based membranes have been selected because of their high hydrogen permeance and selectivity compared to other materials. The gas separation prototype consists in three parts: 1) the feed section, where the blend prepared in the admixture system of the R&D platform is delivered at high pressure to the membrane module, 2) the membrane reactor, where the membranes are allocated and the operating temperature of 400°C is achieved with an oven and 3) an analysis section to check the composition and quantity of the separated flows.

The prototype consists in a feeding line as inlet and two outlets (permeate and retentate). The permeate is the stream rich in hydrogen, and the retentate, rich in methane. A back-pressure regulator is placed at the outlet of the retentate side to set the required trans-membrane pressure difference. The retentate and the permeate lines are connected to the analysis section. It contains mass flow meters to measure and monitor the permeate and retentate flows, which can be analyzed with a gas analyzer.

## D4.2 Report on results of the validation

---

Two different Pd-based membranes have been tested in the prototype. The membrane prototype has only been used for the first experimental campaign with 20/80 %/% H<sub>2</sub>/CH<sub>4</sub> blends and without impurities. In a first experiment the long-term stability of this kind of membranes was tested under a constant feed flow (8.3 NI·min<sup>-1</sup>) and feed pressure (80 bar). In a second round of tests, the feed pressure was varied (10, 20, 40, 60, 80 bar) and then feed flow was tuned for obtaining the maximum H<sub>2</sub> recovery for each feed pressure.

With the first membrane, mixed gas tests were performed at 400 °C feeding 8.33 NI·min<sup>-1</sup> of the H<sub>2</sub>/CH<sub>4</sub> blend (20%mol H<sub>2</sub>) at 80 bar to the membrane module. The mixed gas test consisted in 5 cycles of 100h each, maintain the system at operating pressure but without feed flow between cycles. The permeate flow and hydrogen content in the permeate stream were monitored to assess the gas separation performance of the membranes.

With the second membrane feed flow and pressure were modified between 1.12-6.15 NI·min<sup>-1</sup> and 10-80 bar for the mixed gas tests, respectively, maintaining the operating temperature always at 400 °C. The permeate flow and hydrogen concentration in the permeate stream were monitored to calculate the hydrogen recovery. The whole experiment lasted 175h.

## 4 Results of the first experimental campaign

### 4.1 Gas tightness tests

The tightness of the valves considered in Table 1 has been tested according to the methodology explained in section 3.1. at 80 bar with a 20% mol H<sub>2</sub> blend in CH<sub>4</sub>. The evolution of the pressure and the composition of the gas (%mol H<sub>2</sub>) for each line of the static section during the time of the experiment is given in Figure 4. Two possible losses are possible: i) decrease in pressure level would stand for a critical tightness failure and 2) decrease in the hydrogen concentration in the blend would mean that hydrogen is being lost due to its preferential permeance over methane. There are three lines that allow to discriminate the losses by general parts of the installation. The reference line contains no testing element at all is the blank test. Two other lines include just flanged or screwed couplings. These lines help to distinguish whether a possible leakage comes from the coupling or the body of the valve.

Figure 4 shows no critical pressure losses in any branch of the static section. The pressure oscillates slightly ( $76.7 \pm 4.5$  bar is the biggest interval for the line with flanged ball valves). It is due to temperature changes from day to day, as well as between night and day. The hydrogen content remains basically constant in the three reference lines, being the oscillation shown within the measuring error of the analyzer ( $< 1\%$  mol) and in all cases below  $0.5\%$  mol. Neither the line itself nor the couplings (flanged or screwed) show relevant hydrogen losses and the whole system can be considered tight. The same behavior was observed for the lines with test valves installed. The exception are the lines with ball and needle screwed valves. As the branch with only screwed couplings does not show a measurable hydrogen loss, the decrease in hydrogen concentration observed in the lines with testing valves must occur through the body of these valves. Based on the dimensions of the line (17.2 L volume), the total average leakage rate of hydrogen in both lines was  $2.9 \text{ NmL}\cdot\text{h}^{-1}$ , meaning below  $1 \text{ NmL}\cdot\text{h}^{-1}$  per valve if the same rate for all of them is considered. These losses are negligible and not critical at all. In any event, the installation of screwed caps or connecting a device (e.g. manometers) can solve the problem. It is strange to find these valves unconnected in gas pipelines, except in vent lines. All the valves tested in this campaign can be therefore considered ready for operation under the hydrogen blend studied due to the minimal leakages found.



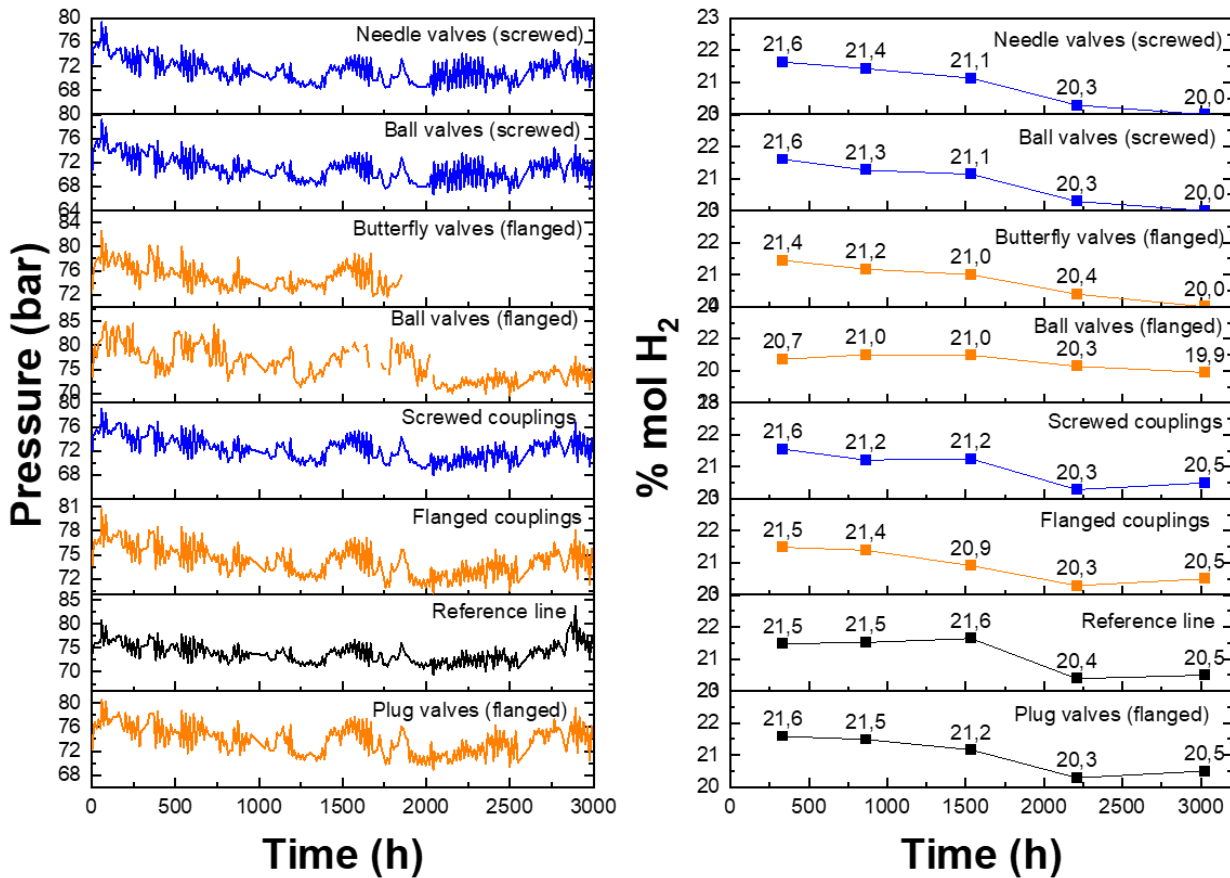


Figure 4. Evolution of the pressure (left) and gas composition in %mol H<sub>2</sub> (right) in each line of the static section during the first experimental campaign

## 4.2 Hydrogen sensitivity tests

### 4.2.1 API 5L constant strain specimens

Test specimens were located inside the pig trap in the loop experimental platform at FHA and exposed from 22/10/2021 to 28/02/2023 (approximately 3070 hours) to a gas atmosphere composed of 80%CH<sub>4</sub>+20%H<sub>2</sub>. The initial gas pressure was established in 80 bar and dynamic flow conditions were applied. After the compressor failure, (10 days after the start of the campaign) the pressure in the loop dropped to 60 bar. This pressure was maintained for 1 month (from 5/11/2021 to 7/12/2021), when it was raised again to 80 bar. From this moment on, the platform was operated in a static mode. At the conclusion of the test, the dynamic section of the loop was depressurized and purged with nitrogen and the pig trap was open. Figure 5 shows the aspect of the racks with the steel specimens inside the pig trap. At the time of opening, no corrosion was observed on the steel samples. Once the outside air entrances in the pig trap, and due to the existing humidity -probably due to the hydrostatic test-, a slight corrosion is produced in the steel specimens.



**Figure 5. Test specimens inside the pig trap in the loop experimental platform at FHA at the beginning of the test, and once concluded**

### **C-ring specimens**

Figure 6 shows the appearance of the tested C-ring specimens. Shallow red spots of corrosion were observed, attributed to the entrance of air inside the pig trap, at the conclusion of the test. No cracks were detected after optical inspection with a LEICA S9i stereo microscope. Metallographic sectioning confirms the absence of cracks both in base and C-ring notch samples (Figure 7).



**Figure 6. Detail of tested C-ring specimens**



## D4.2 Report on results of the validation

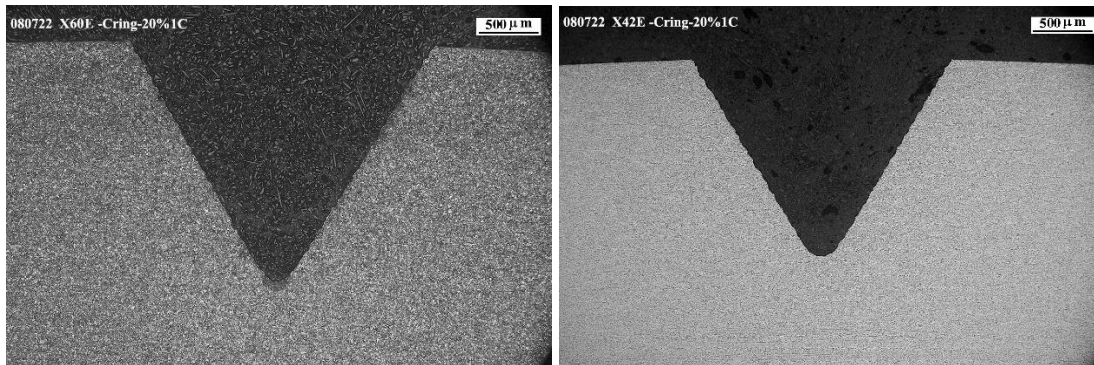


Figure 7. Optical micrographs of notched C-ring sections from steel grades X70 (left) and X42 (right)

### 4pb specimens

Figure 8 shows the appearance upon reception in TECNALIA of welded X70 steel 4pb specimens supported in the loading jig. No cracks were detected during the inspection with a stereo microscope. In 4pb specimens and if no cracks are detected, ASTM G39 suggests carrying out longitudinal sectioning at two locations, typically at 1/3 and 2/3 of width, followed by metallographic preparation and examination performed by optical and scanning electron microscopy (SEM). Metallographic sectioning confirms the absence of cracks in the base, heat affected zones (HAZ) and weld metal areas.

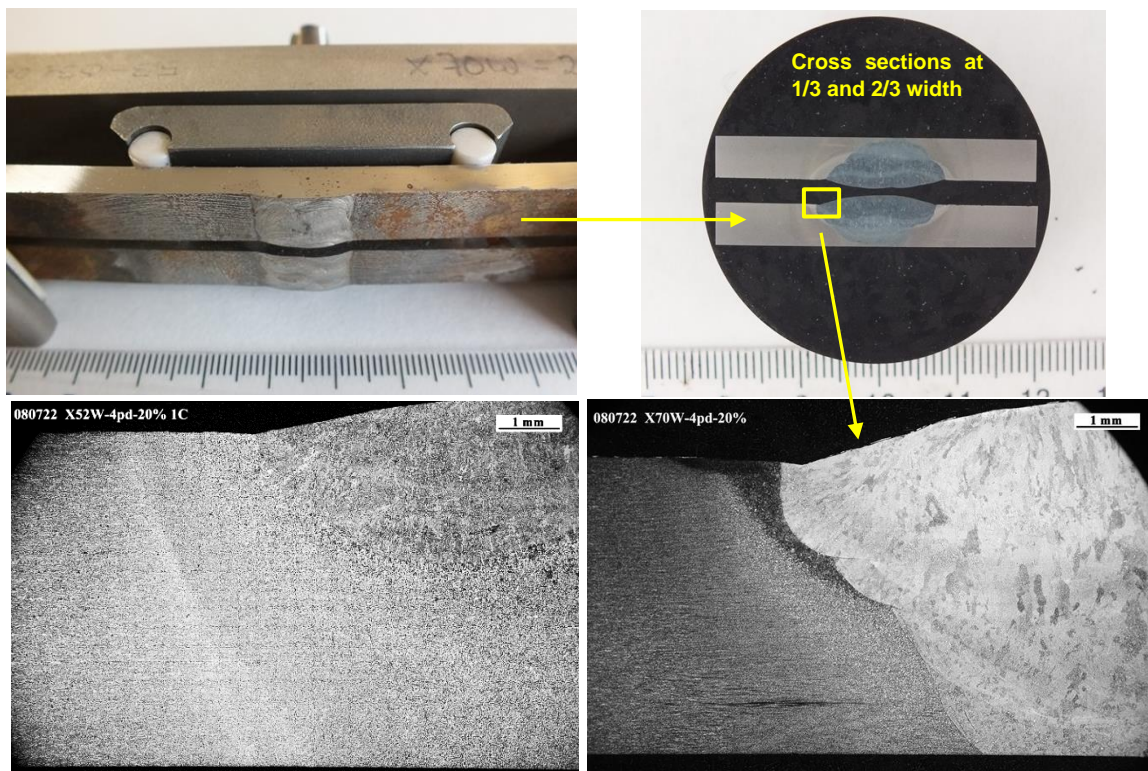


Figure 8. (Up-left) detail of 4pb X70 welded steel specimens; (up-right) metallographic probe of welded sections; (down) optical micrographs of welded joints from steel grades X52 (left) and X70 (right)

### CT-WOL specimens

## D4.2 Report on results of the validation

Figure 9 shows the appearance of the rack with the tested CT-WOL specimens. The CT specimens were unloaded (removing the bolt) and then heat tinted (30 min at 300 °C) and broken in order to evaluate if the initial fatigue pre-crack (generated in air before exposing the specimen to the hydrogen blend) did or did not grow. The fracture surface was examined by SEM microscopy. Measurements of the crack front extent were carried out in three positions. No hydrogen crack growth was measured for any CT-WOL specimen (crack propagation <0.25mm). Fracture surface examination reveal the same fracture mode in the fatigue pre-crack and in the crack front (Figure 10). Results for the CT-WOL specimens testing are summarized in Table 6.

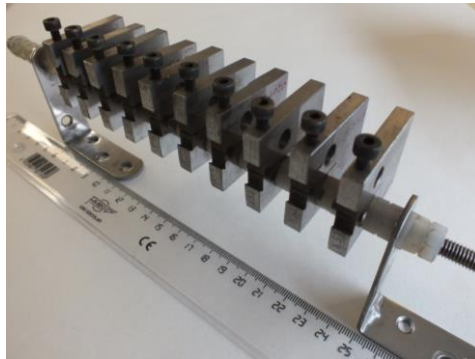


Figure 9. Detail of rack with tested CT bolt loaded specimens

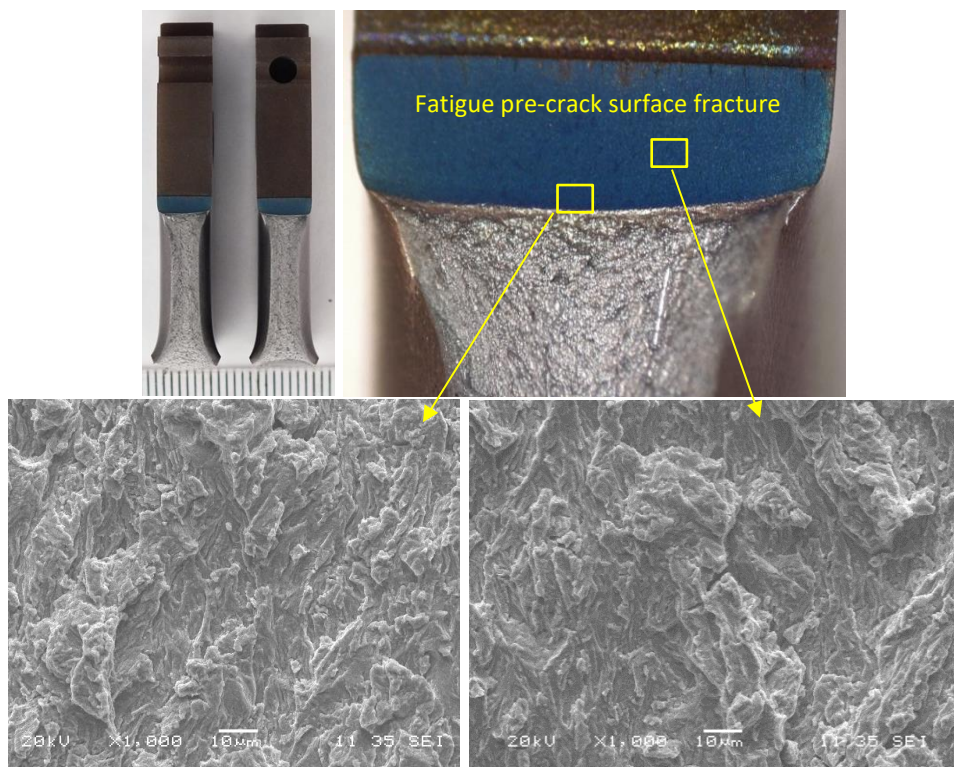


Figure 10. (Up left) two heat tinted fracture surfaces in a X70 CT-WOL tested specimen; (up right) detail of the tinted fatigue precrack; SEM micrographs of the fracture surface in the fatigue pre-crack and in the crack front



Table 6. Results of CT-WOL specimens testing

Campaign number	Gas atmosphere /pressure	Steel grade (number of specimens)	Test duration (hours)	Notch position / crack plane orientation	Crack propagation after exposition	Applied initial stress intensity ( $K_{IAPP}$ ) in MPam <sup>1/2</sup>
1	20%H <sub>2</sub> /80%CH <sub>4</sub> 80 bar	X52 (3)	3070	Base / TL	<0.25mm	32
		X52 HAZ(2)		HAZ / TL	<0.25mm	32
		X70 (3)		Base / TL	<0.25mm	41
		X70 HAZ (2)		HAZ / TL	<0.25mm	41

As shown in Table 6, applied  $K_{IAPP}$  values are lower than those estimated in Table 4. A WOL specimen geometry modification is proposed for future tests in order to be able to use higher  $K_{IAPP}$  values.

### 4.2.2 Inspection of equipment from the dynamic section

The pilot-operated pressure regulator, cartridge filter and turbine flow meter tested in the dynamic section of the testing platform, were disassembled and their different parts (membranes, O-rings, filters, etc.) sent to TECNALIA for inspection. Information regarding the valves and equipment under study was provided in Table 2.

A visual inspection of the items under study was carried out by TECNALIA, with the aid of a stereo microscope with a camera, to detect cracking or other type of hydrogen damage (blistering, for example). There were observed “damaged” areas, principally due to linear or scratch abrasion in certain components, but apart from this, no clear signs of hydrogen damage were observed on the different parts inspected. Only in the case of the membrane regulator it cannot be excluded the possibility of blistering due to hydrogen trapped inside polymer cavities (see Figure 11). Once the component is removed from hydrogen exposure, the blisters can gradually disappear after few days, so it is difficult to make a clear statement.

Figures 11 to 19 show the general appearance and some more detailed analysis of some of the examined items.

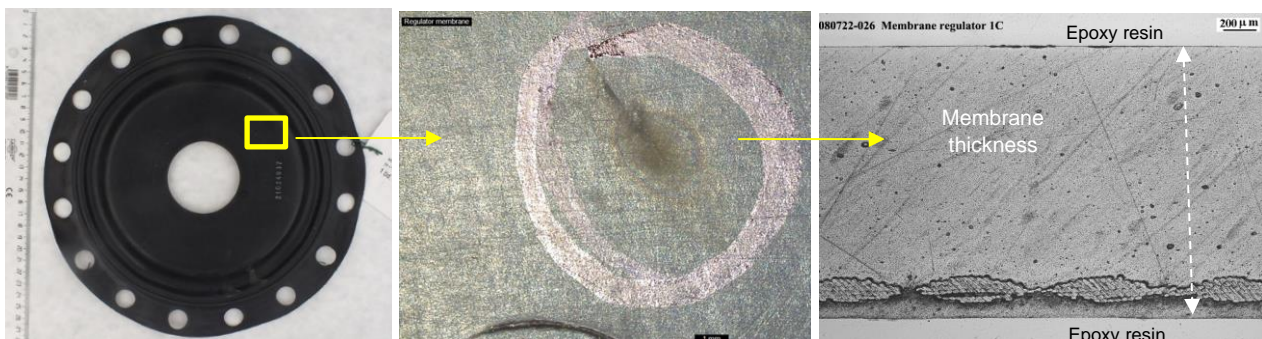


Figure 11. Parts of the pressure regulator: membrane: general appearance (left), detail of area with unknown damaged area (center) and cross section materialographic probe (right) showing a very superficial damage

D4.2 Report on results of the validation

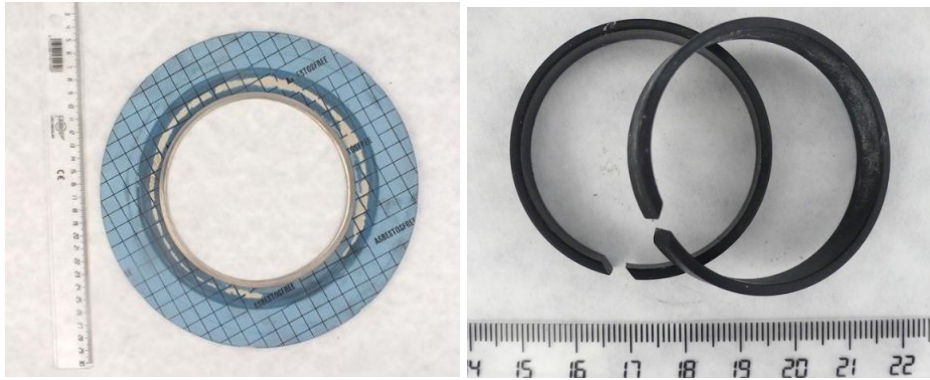


Figure 12. Parts of the regulator: gasket (left) and guide rings (right)

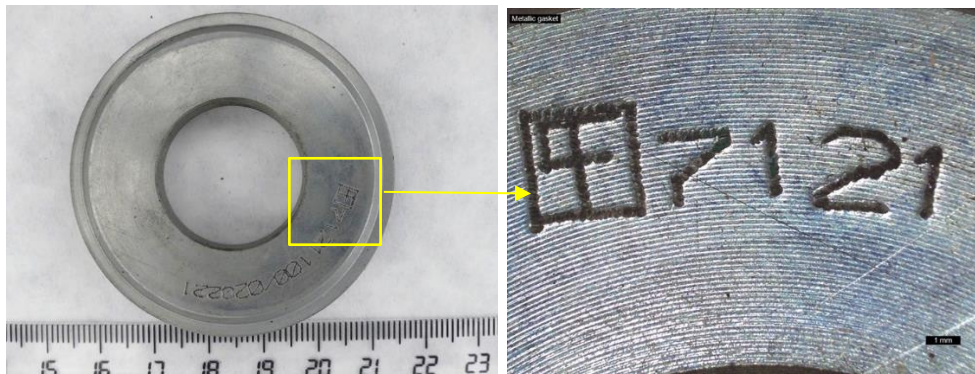


Figure 13. Parts of the regulator: metallic gasket



Figure 14. Prepilot: O-ring (left), filter cartridge (center) and pad (right)



D4.2 Report on results of the validation

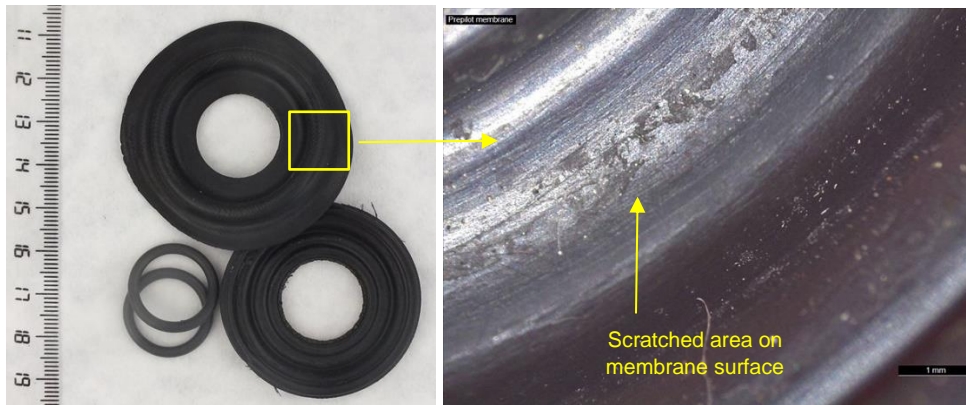


Figure 15. Pilot: membranes and guided rings (right) and detail of membrane

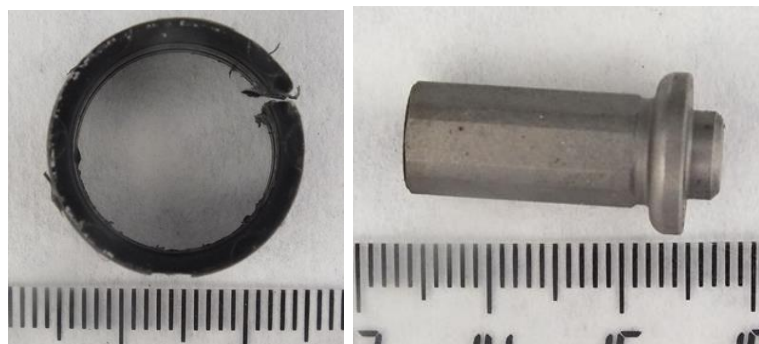


Figure 16. Pilot guide ring (left) and pilot metallic obturator

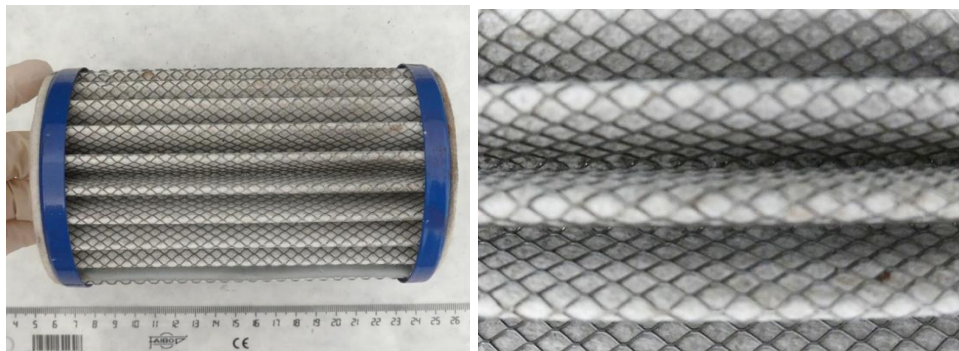


Figure 17. Filter cartridge



Figure 18. Spirometallic gaskets

### 4.2.3 Inspection of equipment from the static section

The main body of the plug, ball and butterfly valves (flanged coupling), present in the static section of the R&D platform, have been disassembled at the end of the test, and inspected to detect signs of hydrogen damage.

In general, the seals of both butterfly and ball valves made of Teflon, do not show any significant damage, except that which may have been generated in the process of disassembling of the valve. The seal bodies made of what appears to be Graphoil, are shown in many cases broken or fragmented, most probably due to the process of dismantling of the valve, as it is a very soft and flexible material. Figures 20 to 23 show the general appearance of some of the examined items.



Figure 19. Butterfly valve seal



Figure 20. Flanged ball valve C-V-17. Detail of teflon seals (left) and graphoil body seals (center and right)



Figure 21. Detail of teflon and graphoil seals in flanged ball valve C-V-15 (left) and C-V-16 (right)





Figure 22. Detail of teflon and graphoil seals in DIDTEK butterfly valve seal

### 4.3 Gas separation performance of the membrane prototype

The separation of the 20/80 (%mol)  $H_2/CH_4$  blend was performed with a gas separation prototype that used Pd-based membranes. The gas separation performance of the prototype with Membrane #1 for the 500h operation is shown in Figure 23.

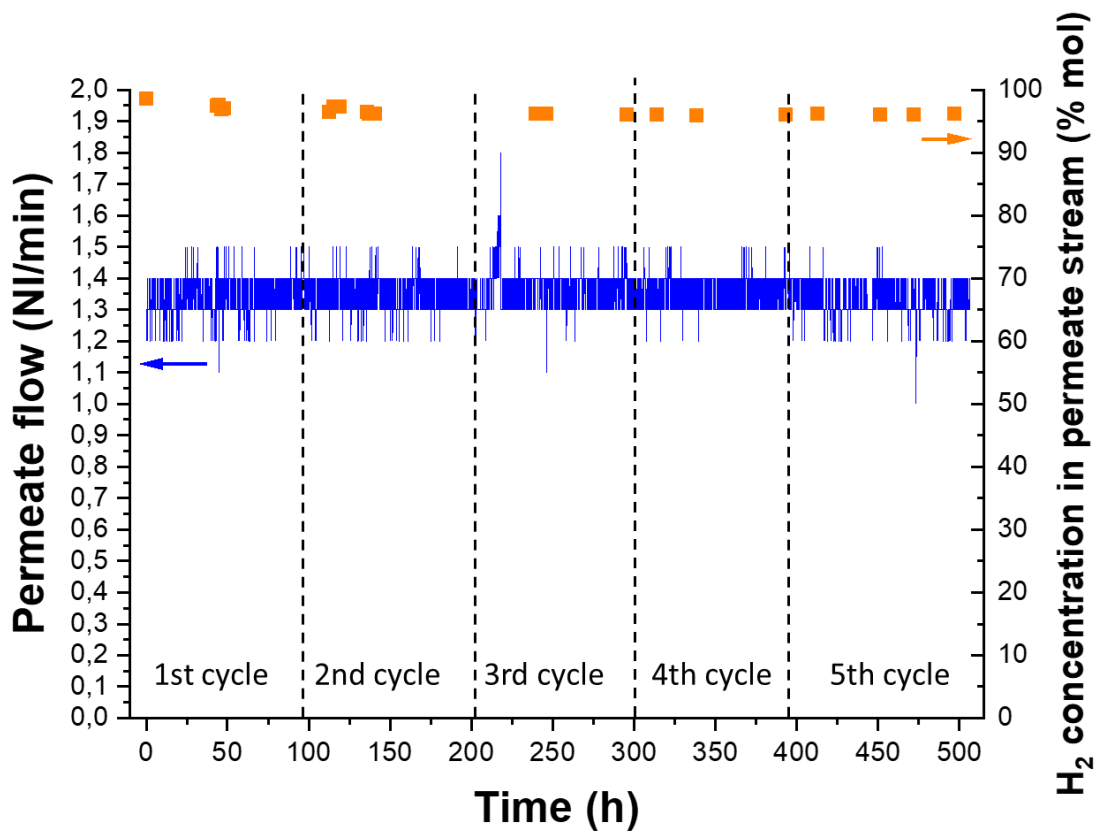


Figure 23. Gas separation performance of the prototype with Membrane #1. Blue line stands for the total permeate flow and orange scatter stands for the  $H_2$  purity in the permeate stream.

## D4.2 Report on results of the validation

The permeate flow (rich in hydrogen) has been monitored and its composition analyzed periodically during the different cycles of the test. Figure 23 shows how the permeate flow remains mainly constant during the whole operation, with an average value of  $1.35 \pm 0.06$  NI·min<sup>-1</sup>. The hydrogen content in the permeate stream is of 98.6 %mol at the beginning of the test but decreases gradually from the second cycle on. Its values are anyway always above 96.0 %mol. The retentate stream can be calculated with a mass balance because the composition of the feed and permeate flows is known. A retentate flow of 6.93 – 7.03 NI/min with a hydrogen content between 3.5 and 5.7%mol can be calculated. The CH<sub>4</sub> content in the retentate flow (between 94.3-96.5%mol) may be sufficient for end-users demanding a high natural gas quality. In any event, the CH<sub>4</sub> content in the retentate stream could be increased increasing the membrane area if deemed necessary.

Gas separation tests were also performed with Membrane #2. Firstly, the feed flow was maintained at 8.3 NI/min and feed pressure was varied (Table 7 – Top). Then, the feed flow was modified for each feed pressure during the test to tune the permeate stream towards obtaining the maximum hydrogen recovery possible (Table 7 – bottom). The permeate flow (rich in hydrogen) was monitored and its composition analyzed periodically during the different cycles of the test. The obtained results about H<sub>2</sub> content in the retentate and permeate streams and hydrogen recovery are summarized in Table 7. The decrease of the feed flow maintaining the feed pressure increases the hydrogen flow in the permeate subsequently increasing the hydrogen recovery rate and reducing the hydrogen content in the retentate stream. The hydrogen purity in the permeate stream was higher than 99.5% after the 175 hours of the testing campaign and, therefore, a hydrogen concentration value down to 2.7% is achieved in the retentate stream when tuning the operating conditions. This is the highest hydrogen recovery value obtained (i.e. 90.0%).

**Table 7. Gas separation performance of the Membrane #2 for the tests under: (top part) same feed flow and variable feed pressure; (bottom part) variable feed flow and feed pressure with the aim at maximizing the hydrogen recovery factor**

Total feed flow (NI/min)	Feed pressure (bar)	%H <sub>2</sub> permeate	%H <sub>2</sub> retentate	%H <sub>2</sub> recovery
8.30	10	99.9	14.9	30.1
8.30	20	99.8	10.3	54.1
8.30	40	99.6	7.8	66.0
8.30	60	99.5	6.6	71.9
8.30	80	99.5	5.3	77.9
Total feed flow (NI/min)	Feed pressure (bar)	%H <sub>2</sub> permeate	%H <sub>2</sub> retentate	%H <sub>2</sub> recovery
1.12	10	99.8	12.2	44.6
2.24	20	99.8	7.6	66.9
3.12	40	99.6	4.8	79.9
4.63	60	99.5	3.4	85.9
6.15	80	99.5	2.7	90.0

## 5 Results of the second experimental campaign

This section contains preliminary results of the second experimental campaign developed in the HIGGS' R&D platform. This campaign ended the 26<sup>th</sup> of September 2022 and so far only the results of the gas tightness tests are available. The results of the hydrogen sensitivity test have still to be analyzed because the characterization of materials is pending and will be included in D4.3. The steps in the experimental campaign are detailed in Table 8.

Table 8. Schedule of the experimental campaign

CAMPAIGN	2021			2022												2023												
	Oct	Nov	Dec	Jan	Feb	Mar	Abr	May	Jun	Jul	Ago	Sep	Oct	Nov	Dic	Jan	Feb	Mar	Abr	May	Jun	Jul	Ago	Sep	Oct	Nov	Dic	
1																												
20% $H_2$ /80% $CH_4$																												
Characterization																												
Transition																												
2																												
20% $H_2$ /80% $CH_4+H_2S+CO_2$																												
Characterization																												
Transition																												
3																												
30% $H_2$ /70% $CH_4(+H_2S+CO_2?)$																												
Characterization																												
Transition																												
4																												
100 % $H_2$																												
Characterization																												

The second experimental campaign has consisted in exposing the testing materials (steels, valves an equipment) to a  $H_2/CH_4$  atmosphere at 80 bar, where the hydrogen level was 20%mol and impurities of  $H_2S$  and  $CO_2$  have been incorporated to the blend, with levels up to 11 ppmv and 4%mol, respectively. As explained in D3.4, these amounts correspond to the maximum concentration of these impurities in natural gas according to the current regulation in Germany [10] and Spain,[11] showing the highest  $CO_2$  and  $H_2S$  levels in natural gas, respectively.

### 5.1 Results of gas tightness tests

The tightness of the valves considered in Table 1 has been tested according to the methodology explained in section 3.1.at 80 bar with the 20% mol  $H_2$  blend in  $CH_4$  including the  $H_2S$  and  $CO_2$  impurities. The evolution of the pressure and the composition of the gas (%mol  $H_2$ ) for each line of the static section during the time of the experiment is given in Figure 24. After the first experimental campaign a temperature transmitter was incorporated to the R&D platform to improve the results of the static section. The quotient between pressure and the product of temperature and compressibility factor must remain constant in a close system as long as no gas flows out of the system. This is why  $P/Z \cdot T$  versus time is also plotted in Figure 24 (middle) to check the evolution of this relationship during the experiment, which can assess the real tightness of the system avoiding the pressure oscillations due to changes in ambient temperature. The compressibility factor has been calculated using the API Soave-Redlich Kwong equation of state for each pressure and temperature value registered by the transmitters in the platform:

$$P = \frac{RT}{v - b} - \frac{a}{v(v + b)}$$

With

$$a_i = a_i(T_{ci})\alpha(T_{ri}, \omega_i)$$

$$a_i(T_{ci}) = \frac{\Omega_a R^2 T_{ci}^2}{P_{ci}}$$

$$\Omega_a = 0.42747$$

## D4.2 Report on results of the validation

For all gases:

$$\alpha(T_{ri}, \omega_i) = [1 + (0.48508 + 1.55171\omega_i - 0.15613\omega_i^2)(1 - \sqrt{T_{ri}})]^2$$

and specially for hydrogen:

$$\alpha(T_{ri}, \omega_i) = 1.202e^{-0.30288T_{ri}}$$

$$b_i = \frac{\Omega_b RT_{ci}}{P_{ci}}$$

$$\Omega_b = 0.08664$$

And the mixing rules:

$$a = \sum_{i=1}^c \sum_{j=1}^c y_i y_j a_{ij}$$

$$a_{ij} = (1 - k_{ij}) \sqrt{a_i a_j}$$

$$b = \sum_{i=1}^c y_i b_i$$

This modification of the SRK EOS has been recommended by the American Petroleum Institute (API) for mixtures of hydrogen with hydrocarbons [12].

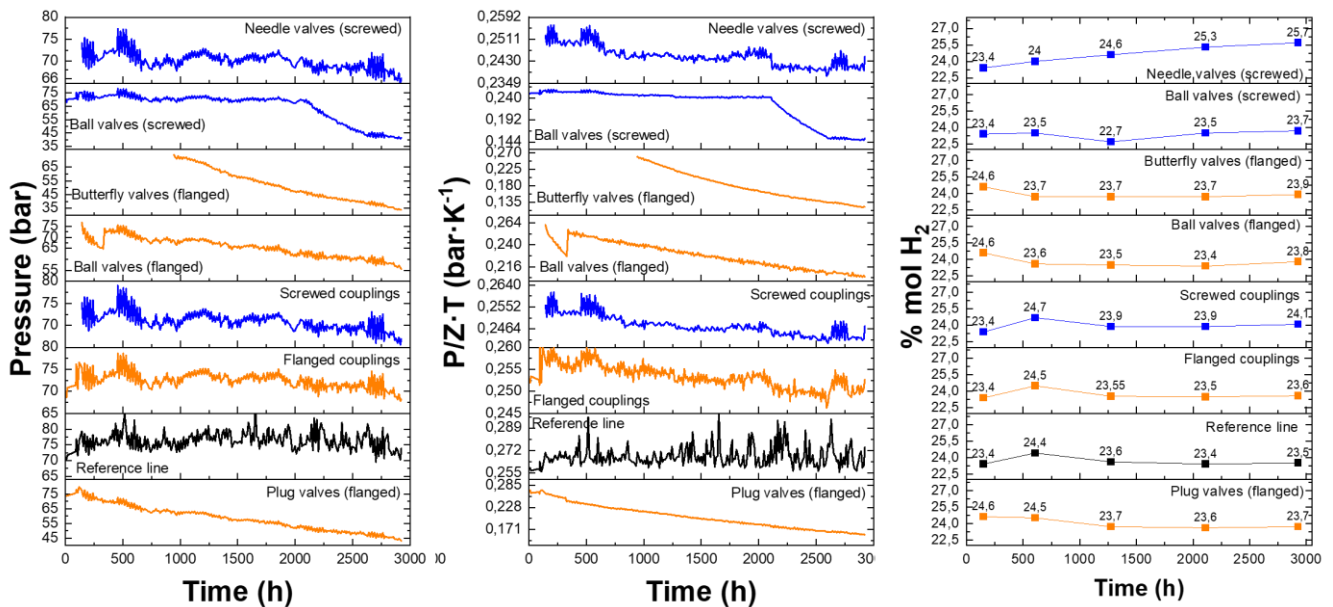


**Figure 24. Evolution of the pressure (left), the P/Z-T quotient (middle) and gas composition in %mol H<sub>2</sub> (right) in each line of the static section during the second experimental campaign**

It can be seen in Figure 24 how neither of the flanged valves (plug, ball or butterfly) remain tight during the test, with gradual pressure losses during the whole time. These valves were disassembled after the first experimental campaign and reassembled again with spare parts. The works performed on them must have not been efficient enough to ensure the tightness of the valves, because they

## D4.2 Report on results of the validation

---

were tight in the first experimental campaign and no damage on their sealing parts was detected after visual inspection. It can be concluded, therefore, that any manipulation on this kind of components should be done only by the manufacturer or a stakeholder with really specialized knowledge. The three lines for blank tests (the branch with nothing installed in it and those containing flanged and screwed couplings) can be considered tight, since no critical P/Z·T drop nor decrease in hydrogen concentration can be detected. Noteworthy, the slight decrease in P/Z·T values correspond to the losses that took place when gas samples were taken outside the system for analysis (standard deviation  $<0.002 \text{ bar}\cdot\text{K}^{-1}$  between analysis points for the lines with flanged and screwed couplings and  $<0.01 \text{ bar}\cdot\text{K}^{-1}$  for the reference line, leading to CVs of 0.006 and 0.035, respectively). The hydrogen concentration in all these lines can also be considered constant during the 3000h that the test lasted, with slightly fluctuating values around 24.5%mol coherent with the measuring error range of the gas analyzer.

In the case of the lines containing ball or needle valves as testing components, the P/Z·T relationship can also be considered constant during the test (standard deviation  $<0.002 \text{ bar}\cdot\text{K}^{-1}$  and CVs $<0.008$ ). There is an exception in the line containing ball valves, where a clear drop in the values can be seen for times between 2100 and 2600 h. This fact is due to a leak in the analysis port in this line. It occurred after one analysis but was not detected and solved until sometime later, leading to the decrease in pressure and P/Z·T values shown in the graph. While the hydrogen concentration in the line with ball valves remains basically constant during the test ( $23.4\pm 0.4 \text{ \%mol}$ ), it is surprising to see how the concentration in the line with needle valves increases constantly as time passes. This tendency is contrary to that found in the experimental campaign. No logical explanation has been found. It is expected to provide a better explanation in the following deliverable. Besides, during periodical inspections with electronic gas detectors, small gas leakage was detected in the testing ball valves. These losses are due to internal leakages and are not sufficient enough to provide a critical pressure drop in the line. This issue not found for the needle valves.

Finally, a critical gas leakage was detected in one the testing ball valves at the end of the campaign. Despite being all the valves tight during the test, this failure occurred after the emptying and inertization process. This specific valve will be characterized to check if it has suffered hydrogen damage and is therefore not compatible for hydrogen service. The results will be given in D4.3.

## 6 Conclusions

The tolerance towards hydrogen of 1) API 5L steels grades X42, X52, X60 and X70, 2) valves (ball, plug, butterfly and needle types), 3) fittings (flanged and screw couplings) and 4) equipment (filters, pressure regulators and gas meters) has been evaluated in the first experimental campaign carried out in the HIGGS' R&D platform built at FHA during WP3. This campaign has considered a gas blend made of H<sub>2</sub>/CH<sub>4</sub> with 20% mol H<sub>2</sub> content, without impurities, at 80 bar and has lasted around 3000 h. Gas tightness tests of representative valves, constant strain tests of API5L steel specimens and gas separation tests with a Pd-based membrane prototype, have been carried out during this campaign.

Most of the testing valves remained tight over 3000h, with just minor hydrogen losses due to hydrogen preferential permeation through the body of screwed ball and needle valves. The visual inspection of the cartridge of the filtering unit and the main parts of the pressure regulator no apparent damage on the different parts was detected, although it is possible that the membrane of the regulator may have suffered blistering. Regarding the steels, the strained C-Ring and 4pb specimens showed no effect of cracking or embrittlement after visual inspection of surface and cross-section, neither in the base material, the heat affected zone, nor the welded material. No crack propagation could be noticed in CT-WOL specimens either, being the extension of the crack below the limits of acceptance of the standard.

Preliminary results of tightness tests of the second experimental campaign (20/80 (%/%vol) H<sub>2</sub>/CH<sub>4</sub> blend with up to 11 ppmv of H<sub>2</sub>S and 4%mol CO<sub>2</sub> as impurities) are also included in this report. The tightness of flanged testing valves was not possible to assess, because after manipulating these valves at the end of the first experimental campaign they did not remain in their original state, concluding that any manipulation on this kind of components should be done only by the manufacturer. The tightness of the flanged and screwed couplings and of the screwed testing valves could also be observed in the test (maximum CV of the P/Z-T <0.008), and they seem compatible with hydrogen under the conditions tested. However, a failure found in one screwed ball valve after emptying the platform makes necessary its full characterization to reach better conclusions, which will be provided in the next deliverable.

Finally, the gas separation experiments with the Pd-based double-skinned membrane prototype showed great gas separation performance. The long-term stability experiment of Membrane #1 led to a good gas separation performance, where the prototype showed a stable permeate flow during the 500h operation with a hydrogen purity over 96%. In the case of Membrane #2, feed flow and feed pressure were tuned to obtain the maximum hydrogen recovery possible, reaching 90% at 80 bar feed pressure and 6.15 NI·min<sup>-1</sup> feed flow with the lowest H<sub>2</sub> content in the retentate of 2.7%, and H<sub>2</sub> purities in the permeate higher than 99.5% after 175h operation. These results show that the membrane technology is promising for the H<sub>2</sub> recovery and purification of low H<sub>2</sub>-concentrated gas streams.



## Bibliography and References

- [1] ISO 6892, Metallic materials - Tensile testing - Part 1: Method of test at room temperature. ISO 6892-1(2019)
- [2] ISO 7539-5, Corrosion of metals and alloys. Stress corrosion testing. Part 5: Preparation and use of C-ring specimens. ISO 7539-5 (1989)
- [3] ASTM G38, Standard practice for making and using C-Ring stress-corrosion test specimens. ASTM G38-01(2021)
- [4] ISO 7539-2, Corrosion of metals and alloys. Stress corrosion testing. Part 2: Preparation and use of bent-beam specimens. ISO 7539-2 (1989)
- [5] ASTM G39, Standard practice for preparation and use of bent-beam stress-corrosion test specimens. ASTM G39-99(2021)
- [6] ASTM E1681, Standard test method for determining threshold stress intensity factor for environment-assisted cracking of metallic materials. ASTM E1681-03(2008)
- [7] ISO 7539-6, Corrosion of metals and alloys. Stress corrosion testing. Part 6: Preparation and use of precracked specimens for tests under constant load or constant displacement. ISO 7539-6 (2018)
- [8] ASTM E399, Standard test method for linear-elastic plane-strain fracture toughness of metallic materials. ASTM E399 (2022)
- [9] A. Arratibel, A. Pacheco Tanaka, I. Laso, M. van Sint Annaland, F. Gallucci. Development of Pd-based double-skinned membranes for hydrogen production in fluidized bed membrane reactors, *Journal of membrane science*, Volume 550, 15 March 2018, Pages 536-544
- [10] D. V. d. G.-. u. W. (DVGW), *DVGW G 260 (A) Technische Regel-Arbeitsblatt: Gas Quality*, 2021
- [11] T. y. C. G. d. E. Ministro de Industria, *Protocolo de detalle PD-01 "Medición, Calidad y Odorización de Gas" de las normas de gestión técnica del sistema gasista*, 2012.
- [12] API Technical Data Book: General properties & characterization. American Petroleum Institute, 7E (2005)

## Acknowledgements

This project has received funding from the Fuel Cells and Hydrogen 2 Joint Undertaking (now Clean Hydrogen Partnership) under Grant Agreement No. 875091 'HIGGS'. This Joint Undertaking receives support from the European Union's Horizon 2020 Research and Innovation program, Hydrogen Europe and Hydrogen Europe Research.

